Nanosize Effects on Hydrogen Storage in Palladium

Miho Yamauchi,*,†,‡ Ryuichi Ikeda,§ Hiroshi Kitagawa,†,§ and Masaki Takata||

Department of Chemistry, Faculty of Science, Kyushu University, Hakozaki 6-10-1, Higashi-Ku, Fukuoka 812-8581, Japan, JST, PRESTO, 4-1-8, Kawaguchi-shi, Saitama 332-0012, Japan, JST, CREST, 4-1-8, Kawaguchi-shi, Saitama 332-0012, Japan, and Structural Science Laboratory, RIKEN SPring-8 Center, Sayo-gun, Hyogo 679-5148, Japan

Received: October 29, 2007; In Final Form: December 12, 2007

The size dependencies of the hydrogen-storage properties in polymer-coated Pd nanoparticles with diameters of 2.6 ± 0.4 and 7.0 ± 0.9 nm were investigated by a measurement of hydrogen pressure-composition isotherms. Their storage capacities per constituent Pd atom in the particles decreased with decreasing particle size, whereas the hydrogen concentrations in the two kinds of nanoparticles were almost the same and 1.2 times as much, respectively, as that in bulk palladium after counting zero hydrogen occupancy on the atoms in the first surface layer of the particles. Furthermore, apparent changes in hydrogen absorption behavior with decreasing particle size were observed, that is, a narrowing of the two-phase regions of solid-solution and hydride phases, the lowering of the equilibrium hydrogen pressure, and a decrease in the critical temperature of the two-phase state. By analyzing the isotherms, we quantitatively determined the heat of formation ($\Delta H_{\alpha\rightarrow\beta}$) and the entropy change ($\Delta S_{\alpha\rightarrow\beta}$) in the hydride formation of the nanoparticle. $\Delta H_{\alpha\rightarrow\beta}$ and $\Delta S_{\alpha\rightarrow\beta}$ for the 2.6 ± 0.4 nm diameter Pd nanoparticle were -34.6 ± 0.61 kJ$(H_2\ mol)^{-1}$ and -83.1 ± 1.8 J$(H_2\ mol)^{-1}K^{-1}$, whereas for the 7.0 ± 0.9 nm diameter Pd nanoparticles the values were -31.0 ± 1.8 kJ$(H_2\ mol)^{-1}$ and -67.3 ± 5.1 J$(H_2\ mol)^{-1}K^{-1}$, respectively. These quantities gave us a prospective picture of hydrogen absorption in Pd nanoparticles and the peculiarities in the formation of a single nanometer-sized hydride.

Introduction

The development of techniques for the use of hydrogen energy is one of the most important energy-related subjects, involving hydrogen generation,[1] storage,[2,3] purification,[2,4] energy conversion from hydrogen to electricity,[5] and so forth. It is well known that some kinds of metals or alloys, which are called hydrogen-storage alloys, are reactive to hydrogen gas and can store hydrogen through chemical bonds between metal and hydrogen atoms.[6] At the present time, even though metals or alloys are the only materials for storing hydrogen above room temperature, their working conditions must be improved for practical usage; for example, the Department of Energy sets the goal for the working temperature for hydrogen-storage systems to be in the range from −40 to 80 °C by the year 2015. As a novel hydrogen-storage material, we considered metal nanoparticles.[7,8] Recently, metal nanoparticles have been found to show many prominent properties, such as surface plasmon, magnetism,[9] catalysis,[10] and so forth, that originate from the large surface fraction in the particles and discreteness of their electronic states. The hydrogen-storage properties of metals are related to chemical reactivity with hydrogen both on the surface and inside the metal. Nanoparticles are expected to show fast kinetics for decomposition/reformation of hydrogen molecules on the metal surface and higher storage density in the inside/outside of the particles. Moreover, thermodynamic stabilities of nanometer-sized hydrides are expected to change because of their limited volume, from those in the bulk state. Therefore, nanoparticles have the potential to show exotic hydrogen absorption properties, giving us many possibilities for discovering new kinds of storage media.

Palladium (Pd) is a classical hydrogen-storage metal and shows exceptional features for practical use; for example, Pd absorbs hydrogen at ambient temperature and pressure.[2,6] Many studies on hydrogen storage in Pd nanoparticles have been published, and several characteristics were ascertained. The phase transition from the solid solution (α phase) of Pd and hydrogen to the hydride (β phase) takes place with an accompanying apparent pressure hysteresis even in particles of 2−3 nm in diameter, and the miscible gap in the hydrogen pressure-composition (PC) isotherm is narrowed. These results imply that hydrogen solubility in the solid-solution phase is increased but decreased in the hydride phase.[7,11−15] Concerning these results, Kirchheim explained that the increase in the solubility in the solid-solution phase is due to the increase in hydrogen solubility in the subsurface region within 0.7−1.1 nm from the surface, while no phase transition to the β phase occurs in this region.[11,15] Alternatively, Eastman concluded on the basis of X-ray diffraction results that the phase transition involves the whole of the nanoparticle, and the narrowing of the two-phase region is brought about by peculiar thermodynamic factors in the nanoparticles.[12] However, a general explanation of the hydrogen absorption mechanism in Pd nanoparticles, especially those that are single nanometer in size, has not been produced because there has not been reliable data for the size dependency in the single nanometer region. One of our purposes in this study is to obtain systematic absorption/desorption data by using Pd nanoparticles that are homogeneous in size and to determine

* Corresponding author. Address: Department of Chemistry, Faculty of Science, Kyushu University, Hakozaki 6-10-1, Higashi-Ku, Fukuoka 812-8581, Japan. Tel: +81-92-642-2319. Fax: +81-92-642-2570. E-mail: mhyamascc@mbox.nc.kyushu-u.ac.jp.

† Kyushu University.

‡ JST, PRESTO.

§ JST, CREST.

|| RIKEN SPring-8 Center.

10.1021/jp710447j CCC: $40.75
Published on Web 02/12/2008

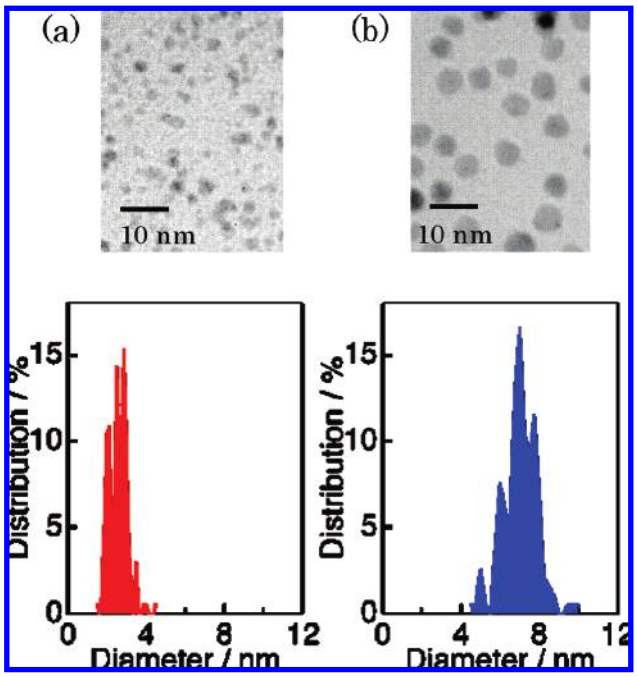

Figure 1. TEM images (upper) and size distributions (lower) of (a) Pd-S and (b) Pd-L.

thermodynamic quantities such as the heat of formation and the entropy change for hydride formation on Pd nanoparticles. Because these quantities are related to both the electronic state[16] and the structural flexibility of the nanometer-sized hydride, we would achieve a clarification of the chemistry in the hydrogen absorption mechanism. Here, we intend to develop the entire story of hydrogen storage in Pd nanoparticles with possible events in the course of size diminution of metal particles.[17]

Materials and Methods

As a target sample for hydrogen absorption/desorption studies, we adopted Pd nanoparticles coated with poly[*N*-vinyl-2-pyrrolidone], abbreviated as PVP. Because PVP does not absorb hydrogen itself, and it binds to metal surfaces without strong interactions, Pd nanoparticles coated with PVP were expected to show their inherent hydrogen-storage properties. Two kinds of nanoparticles with different diameters were prepared by ethanol reduction and continuous stepwise growth.[18] From transmission electron microscope (TEM) images for the synthesized samples, as shown in Figure 1, it was found that Pd nanoparticles homogeneous in size were produced. This marked characteristic allowed us to evaluate the size dependence of the hydrogen-storage properties. The particle diameters in these samples were estimated to be 2.6 ± 0.4 and 7.0 ± 0.9 nm. The samples consisting of small and large particles are hereafter called Pd-S and Pd-L, respectively. It was found from elemental analysis that metal compositions in the products were changed slightly from the values of raw materials; that is, Pd contents in the starting materials for Pd-S and Pd-L are 8.7 and 61 wt %, whereas those in the final products were 11 and 65 wt %, respectively.

The hydrogen absorption/desorption behavior up to a hydrogen pressure of 0.1 MPa of was investigated by the measurement of hydrogen pressure-composition (PC) isotherms using an automatic PC isotherm apparatus (Suzuki Shokan Co., Ltd). Before the measurement, nanoparticles were dried in vacuo at 373 K for 24 h to remove water and exposed to a hydrogen

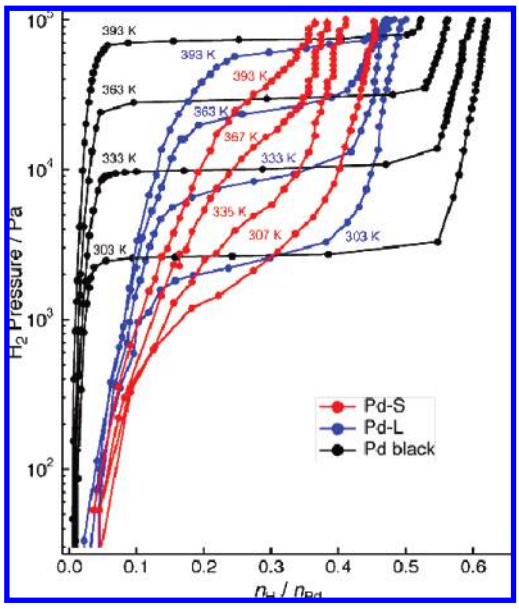

Figure 2. Hydrogen pressure-composition isotherms in absorption processes for Pd-S (red), Pd-L (blue), and Pd black (black).

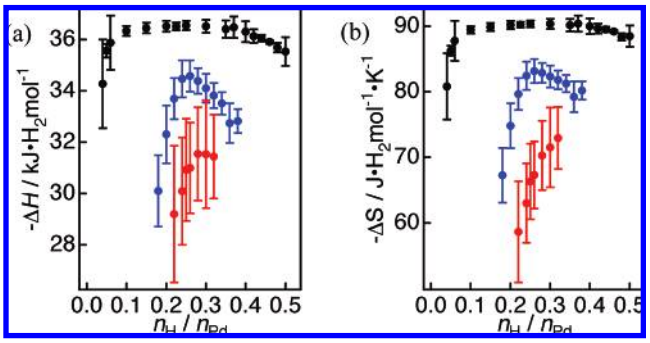

Figure 3. Hydrogen concentration (n_H/n_{Pd}) dependences of (a) heat of formation ($\Delta H_{\alpha\rightarrow\beta}$) and (b) standard entropy ($\Delta S_{\alpha\rightarrow\beta}$) for the phase transition from α to β phase in Pd-L(blue), Pd−S(red) and Pd black-(black). Indicated values are negative ones of $\Delta H_{\alpha\rightarrow\beta}$ and $\Delta S_{\alpha\rightarrow\beta}$.

atmosphere of 2 MPa for 6 h as a pretreatment. Details of the pretreatment have been reported elsewhere.[7] Pd black (Kanto Chemical, Co., Inc) was used in all measurements as a bulk control. Although we evaluated the hydrogen solubility by using the metal composition of the raw materials in the previous report,[7] in the present study we adopted a metal composition determined by elemental analysis for enabling detailed comparison of the solubility between Pd-S and Pd-L. We carried out powder X-ray diffraction (XRD) measurements at room temperature for the two kinds of samples kept under vacuum and 0.1 MPa of hydrogen gas using synchrotron radiation ($\lambda =$ 0.0684938(5) nm at BL-1B in the Photon Factory of the High Energy Accelerator Research Organization, Japan for Pd-S and $\lambda = 0.0511425(2)$ nm at BL02B2 in SPring-8 for Pd-L).

Results

1. PC Isotherms. PC isotherms for the absorption process are shown in Figure 2. The hydrogen solubility is given by molar concentrations of hydrogen per Pd atom for an equilibrium hydrogen pressure. In the isotherm of Pd black, abrupt increases in the hydrogen concentration at a constant hydrogen pressure, namely, pressure plateaus, and pressure hystereses were observed (full PC isotherms with absorption and desorption curves are shown in Figure 7), which

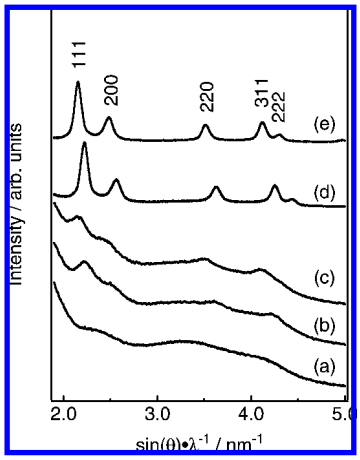

Figure 4. Powder XRD patterns for (a) glass capillary as a blank, Pd-S (b) under vacuum and (c) under 0.1 MPa H_2, and Pd-L (d) under vacuum and (e) under 0.1 MPa H_2. The patterns are drawn for $\sin(\theta)/\lambda$ for comparison of patterns observed using different wavelengths.

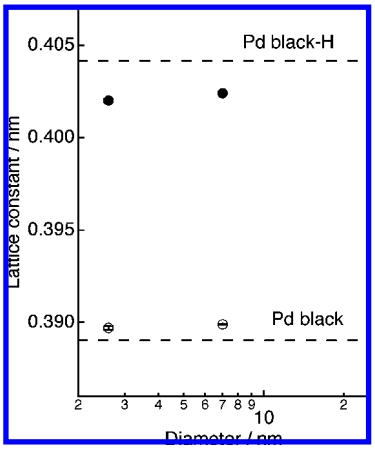

Figure 5. Lattice constants of the particles under vacuum (open circle) and 0.1 MPa H_2 (filled circle) plotted against the diameter of the nanoparticles. The corresponding constants for Pd black are depicted by broken lines.

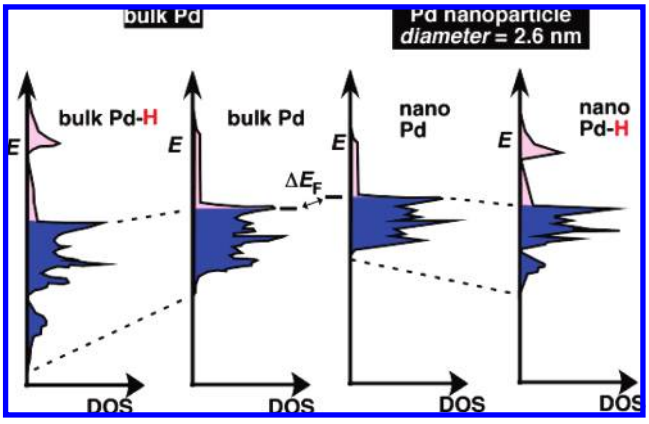

Figure 6. Illustrations of the DOS near the Fermi level in bulk Pd and Pd-S showing size dependence in hydrogen-storage properties. The occupied states are represented by the color blue.

correspond to a miscible state in the phase transition from the α to the β phase. This phase transition is caused by a chemical reaction described by

$$\frac{2}{C_\beta - C_\alpha}\mathrm{PdH}_{C_\alpha} + \mathrm{H}_2 = \frac{2}{C_\beta - C_\alpha}\mathrm{PdH}_{C_\beta} + \Delta H_{\alpha\to\beta} \quad (1)$$

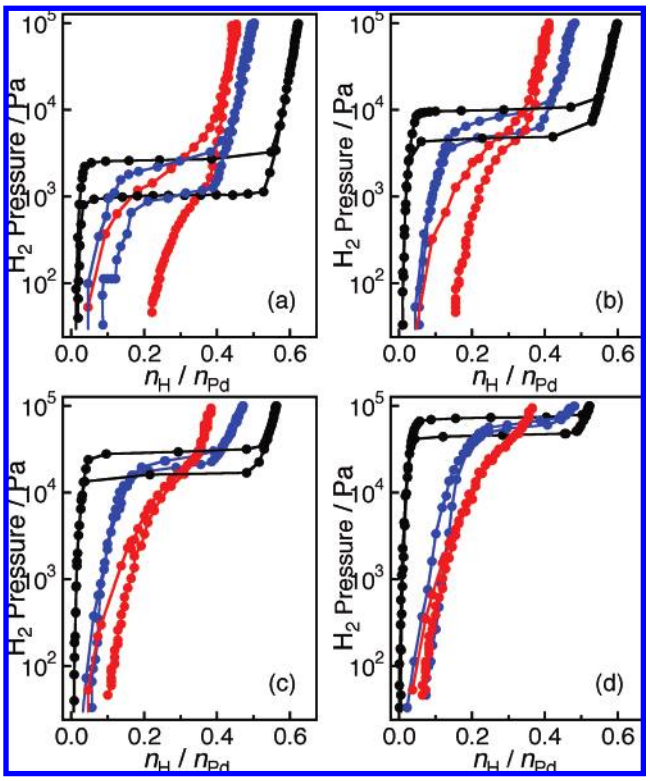

Figure 7. Full PC isotherms in absorption and desorption processes for Pd-S (red), Pd-L (blue), and Pd black (black) measured at (a) 303, (b) 333, (c) 363, and (d) 393 K, while the isotherms for Pd-S were measured at (a) 307, (b) 335, (c) 367, and (d) 393 K.

where $\Delta H_{\alpha\to\beta}$ is the heat of formation and C_α (or C_β) is the maximum (or minimum) hydrogen concentration in the α (β) phase.[19] C_α (C_β) corresponds to the starting (ending) concentration of a miscibility gap. For each isotherm observed in both nanoparticles, a plateau-like region with a certain extent of gradient in equilibrium pressure and with an apparent hysteresis was observed.[7] These plateau-like regions were found inside the corresponding region for Pd black. This phenomenon suggests that the α and β phases coexist, that is, form a miscible state, even in quite small-sized metal particles.[7,11,12,15] It is noteworthy that the gradient of the pressure increase with hydrogen concentration in the miscible regions became steeper with decreasing particle size.

An equilibrium pressure in this region is associated with $\Delta H_{\alpha\to\beta}$ and the entropy change ($\Delta S_{\alpha\to\beta}$) for the phase transition from the α to the β phase. For the case that one mole of hydrogen gas is consumed in this reaction, these thermodynamic quantities are described as follows[20]

$$\ln\frac{P}{P_0} = \frac{\Delta H_{\alpha\to\beta}}{RT} - \frac{\Delta S_{\alpha\to\beta}}{R} \quad (2)$$

where P and P_0 are the equilibrium hydrogen pressure and the standard hydrogen pressure (0.1 MPa), respectively. For all samples, linear relationships were observed between $\ln(P/P_0)$ and $1/T$, indicating that $\Delta H_{\alpha\to\beta}$ and $\Delta S_{\alpha\to\beta}$ are constant in the 303−393 K range. By using eq 2, we determined $-\Delta H_{\alpha\to\beta}$ and $-\Delta S_{\alpha\to\beta}$ corresponding to the exothermic heat and the entropy loss in the reaction, respectively, at several hydrogen concentrations in the miscible region, and show them in Figure 3. It was found that $-\Delta H_{\alpha\to\beta}$ and $-\Delta S_{\alpha\to\beta}$ for the nanoparticles decrease with decreasing particle diameter. In particular, because the $-\Delta H_{\alpha\to\beta}$ value corresponds to the bond strength between Pd

and hydrogen (H) in the β phase, the smaller $-\Delta H_{\alpha\rightarrow\beta}$ for the smaller particle implies that the bond strength of Pd−H becomes weaker with decrease in metal particle size. The $-\Delta H_{\alpha\rightarrow\beta}$ and $-\Delta S_{\alpha\rightarrow\beta}$ values in the nanoparticles depend on the hydrogen concentration, implying that the local structure in the Pd hydride is a little different at the site of the nanoparticles, for example, surface and core portions. In other words, this means that the bond strength of Pd−H is different at the different sites. Therefore, the distribution of the equilibrium pressure in the miscible region is attributable to an inhomogeneous circumstance insides the nanoparticles.

2. Powder XRD. Powder XRD patterns for Pd-S and Pd-L under vacuum and 0.1 MPa of hydrogen (H_2) gas are shown in Figure 4. The diffraction patterns for all samples were ascribed to face-centered-cubic symmetry in the same manner as in the bulk. The diffraction peaks observed for both nanoparticles under H_2 were shifted to lower angles than those under vacuum, indicating that the lattices in the Pd nanoparticles are expanded because of hydrogen absorption. Lattice constants of the nanoparticles with and without hydrogen, determined by a pattern-fitting analysis based on the Le Bail method.[21] Although the lattice constant for Pd-S was already obtained in the previous report,[7] further optimization of the constant was carried out for better quality in the structural analysis by using only the diffraction peaks with an index higher than 0 0 2. The lattice constants determined here are shown in Figure 5. The extents of lattice expansion resulting from hydrogen absorption in Pd-S and Pd-L, that is, differences between the lattice constants under vacuum and a hydrogen atmosphere, were shown to be smaller than that in Pd black.

It is noticeable that the size dependency of the lattice constants under vacuum in Pd nanoparticles showed a tendency opposite of those in 5d metals such as Au and Pt, where lattices of Au and Pt nanoparticles are contracted due to surface effects compared with those in the bulk.[22] At the present stage, we cannot give any reliable reasons for the reverse relation observed in Pd, but we expect that Pd nanoparticles less than 10 nm in diameter cannot be stabilized sufficiently by the metallic cohesion as seen in Pt and Au nanoparticles. In general, electronic clouds of the 4d transition metals, such as Pd, shrink compared with those of 5d metals, such as Au and Pt, so it is possible that the extent of energetic stabilization due to metallic cohesion for Pd is smaller than that for 5d metals. Moreover, the longer interatomic distance of Pd nanoparticles implies an imperfection as a crystalline metal due to the nature of 4d transition metals.

Discussion

1. Hydrogen-Storage Mechanism in Pd Nanoparticles. As a result of various detailed studies on the electronic state of the bulk Pd−hydrogen system,[17,19,23,24] it has been shown that the hydrogen-absorption properties of Pd are closely related to its electronic state. The conduction band of bulk Pd consists of the overlap of high density-of-state (DOS) 4d and broad 5s bands.[25] At low hydrogen concentrations, a discrete energy state is formed below the 4d band resulting from the introduction of a hydrogenic potential between Pd atoms.[24] With further increase in hydrogen concentration, the discrete state grows at the expense of a portion of the conduction band to an energy band situated under the bottom of the 4d band.[24] This band formation makes the total energy for the Pd−H system lower than that for a coexisting state of the solid solution and H_2 gas, causing a phase transition from the α to the β phase.[14] Hydrogen absorption proceeds smoothly up to C_β, where 4d holes are fully occupied.[24] If the heat of formation for the α phase is negligible, then $-\Delta H_{\alpha\rightarrow\beta}$ values are estimated by the difference between the averaged energy for Pd hydride and that for pure Pd.[23]

In Figure 2, C_α values observed for Pd-S at 307 K, Pd-L at 303 K, and Pd black at 303 K were estimated from the intersection of two extrapolated lines around the starting points of the miscible regions to be 0.12, 0.11, and 0.03 H/Pd, respectively, and, from the ending points, C_β were 0.38, 0.43, and 0.55 H/Pd, respectively. Considering the smaller C_β values observed for the nanoparticles, we propose the following model. In the case that their 4d and 5s band widths are narrower compared with those in the bulk, orbital overlappings for band formation are suppressed in the nanoparticles. The number of 4d holes, originating from an overlap between 4d and 5s bands, should be smaller. This expectation is consistent with larger lattice constants of the nanoparticles as discussed above. Pd nanoparticles originally have a small number of empty states in the 4d band, implying the possibility of small C_β values. The downward shift of the metallic band in energy is brought about by the Coulomb interaction between electrons and protons,[19] which is proportional to the squared distance between these charges. Small values of $-\Delta H_{\alpha\rightarrow\beta}$ and small C_β, hence, indicate a small expansion of the electronic cloud, which is equivalent to a narrow bandwidth in the Pd nanoparticles.

The phase transition occurs when the chemical potentials in the α and β phases are the same.[14,26] The large C_α values in nanoparticles imply that the α phase is stabilized in the nanoparticles, and the energetic gain brought about by hydride formation is small compared with that in the bulk. Small $-\Delta H_{\alpha\rightarrow\beta}$ values in the nanoparticle support this explanation. Generally speaking, a large amount of stabilization is obtained in the metallic band formation among orbitals with energy levels close to each other. Small values of $-\Delta H_{\alpha\rightarrow\beta}$ for hydride formation in Pd nanoparticles suggest that at the Fermi level, as it were, the chemical potential in the nanoparticles should be higher than that in the bulk, resulting in a small energetic stabilization for the hydride formation in the nanoparticles. This explanation seems reasonable because nanoparticles less than 10 nm in diameter are considered to be on the way from an atom to the bulk crystal that is stabilized by its cohesive energy more than are atoms. These phenomena are illustrated in Figure 6.

Assuming that the entropy change during the hydride formation comes mainly from the entropy loss of hydrogen gas,[20] small $-\Delta S_{\alpha\rightarrow\beta}$ values in the nanoparticles indicate that hydrogen atoms in nanoparticles possess a relatively large entropy compared with those in bulk Pd. In other words, hydrogen atoms in the nanoparticles retain a part of the freedom in the gaseous state, implying that atomic arrangements in nanoparticles are statically or dynamically disordered. A more important consideration is that a small loss of entropy causes hydride formation under a low hydrogen pressure. This is because even a low hydrogen pressure (on the left-hand side in eq 2) can compensate the entropy loss in the solidification of hydrogen gas (on the right-hand side).

2. Phase Transition in Nanometer-Sized Pd and Hydrogen Systems. Full PC isotherms for both absorption and desorption processes are shown in Figure 7. For all samples, the pressure gap widths in the miscible region observed at 303 K seemed to be similar. With increasing temperature, the gap widths for the smaller nanoparticles became smaller. It has been reported that the pressure hysteresis is brought about by a transformation-induced strain due to the volumetric change in hydride forma-

tion.[26] As mentioned above, differences in the lattice expansion accompanying hydrogen absorption around 303 K were observed, but they do not look large enough to bring a considerable size dependence to the pressure gap. It can be supposed, however, that lattice expansion at temperatures above 303 K may show size dependence, for example, the difference in the lattice expansion for the nanoparticles becomes smaller than that for the bulk with increasing temperature.

It is noted that hysteresis in the PC isotherm for Pd-S disappeared at 393 K. No hysteresis implies that only a single phase is formed in the solid phase, that is, the critical state of the α and β phases is attained.[27] The critical temperature (T_c) in the bulk system is reported to be 565 K.[19,20] Thus, a marked decrease of T_c was found in Pd nanoparticles. Eastman has predicted the lowering of T_c in nanoparticles,[12] but neither experimental studies on analogous behavior nor discussions on its origin have been reported. The question of why the Pd nanoparticles exhibit such unique phase behavior can be answered as follows. The hydride of Pd-S has large entropy compared with the bulk hydride. This is understandable by considering small $-\Delta S_{\alpha\rightarrow\beta}$ values in the nanoparticles shown in Figure 3. Moreover, because the bond strength between Pd and H is weak, as supposed from the small $-\Delta H_{\alpha\rightarrow\beta}$, we can expect that the stabilization energy originating from this weak chemical interaction is not enough for the hydride formation any longer; that is, $\Delta H_{\alpha\rightarrow\beta} > \Delta S_{\alpha\rightarrow\beta}T$.

In this study, any surface effects on hydrogen storage are not considered because it is difficult to evaluate hydrogen-storage capacities for atoms in this region. However, a large percentage of the atoms in nanoparticles are located around the surface; that is, the proportions of surface atoms in the particles are estimated to be 45 and 21 atom % under the assumption that Pd nanoparticles in Pd-S and Pd-L take a cuboctahedral structure made up of 5 atomic shells (ca. 560 Pd atoms in total) and 13 shells (ca. 8200 atoms), respectively. Assuming that the surface atoms after pretreatment are utterly inactive to the repeated hydrogen absorption/desorption[15] hydrogen concentrations inside Pd-L and Pd-S come to be the same and 1.2 times as much as that in bulk Pd, respectively. In the foregoing discussion of composition dependencies of thermodynamic quantities, we reported the presence of a high inhomogeneity in nanoparticles of the hydride. It is, therefore, possible that a domain exists where hydrogen atoms are highly concentrated inside Pd nanoparticles.

Conclusions

We observed a clear size dependence of the hydrogen PC isotherms for Pd nanoparticles that are single nanometer in size. From the isotherms, we determined thermodynamic quantities for hydride formation. To the best of our knowledge, these are the first quantitative data concerning size dependencies for the chemical reaction inside metal nanoparticles. Using the information obtained from PC isotherms together with the derived thermodynamic quantities, we proposed a hydrogen-storage mechanism in Pd nanoparticles. These results imply that hydrogen-storage properties of metals can be controlled by changing their size. It is noticeable that the equilibrium hydrogen pressure drops in the nanoparticle. Because this phenomenon comes from the large degree of freedom in the nanometer-sized materials besides the weak chemical bond in the nanohydride, it is concluded that lowering of the working temperature and pressure is brought about by the inherent nature of the nanoparticles. The hydrogen-storage capacity of Pd decreases with decreasing crystalline size, but it can be hoped that some kinds of alloys may exhibit good performance in hydrogen storage after their size and composition are controlled in the nanometer-sized region.

Another important characteristic of metal nanoparticles is their excellent catalytic abilities. Here, we clarified the size dependency concerning hydrogen storage in Pd; that is, hydrogen atoms are highly concentrated inside Pd nanoparticles with diameters of a few nanometers. This knowledge can be important in the development not only of hydrogen-storage media but also of novel catalysts in hydrogen handling.

Acknowledgment. This work was supported by a Grant-in-Aid for Scientific Research 17750056, a Grant-in-Aid for Scientific Research on Priority Areas (Chemistry of Coordination Space, No. 16074212), a Grant-in-Aid for the Global COE Program, "Science for Future Molecular Systems", a Grant-in-Aid for 21st Century COE Program "Integration Technology of Mechanical Systems for Hydrogen Utilization", and a Grant-in-Aid for Elements Science and Technology Project from the Ministry of Education, Culture, Sports, Science and Technology (MEXT), Fukuoka Industry Science Technology Foundation Grant for Nanotechnology, Sumitomo Foundation Grant for Basic Science Research Projects, and Yoshida Grant Foundation. The synchrotron radiation experiments were performed at the BL02B2 in SPring-8 with the approval of the Japan Synchrotron Radiation Research Institute (JASRI) and at BL-1B in the High Energy Accelerator Research Organization.

References and Notes

(1) (a) Fujishima, A.; Honda, K. *Nature* **1972**, *238*, 37−38. (b) Deluga, G. A.; Salge, J. R.; Schmidt, L. D.; Verykios, X. E. *Science* **2004**, *303*, 993−997. (c) Schmidt, L. D.; Dauenhauer, P. J. *Nature* **2007**, *447*, 914−915. (d) Ozawa, H.; Haga, H.; Sakai, K. *J. Am. Chem. Soc.* **2006**, *128*, 4926−4927.

(2) Graham, T. *Philos. Trans. R. Soc. London* **1866**, *156*, 399.

(3) (a) Chen, P.; Xiong, Z.; Luo, J.; Lin, J.; Tan, K. L. *Nature* **2002**, *420*, 302−304. (b) Ye, Y.; Ahn, C. C.; Witham, C.; Fultz, B.; Liu, J.; Rinzler, A. G.; Colbert, D. K.; Smith, A.; Smalley, R. E. *Appl. Phys. Lett.* **1999**, *74*, 2307−2309. (c) Rosi, N. L.; Eckert, J.; Eddaoudl, M.; Vodak, D. T.; Kim, J.; O'Keeffe, M.; Yaghi, O. M. *Nature* **2003**, *423*, 705.

(4) (a) Kamakoti, P.; Morreale, B. D.; Ciocco, M. V.; Holward, B. H.; Killmeyer, R. P.; Cugini, A. V.; Sholl, D. S. *Science* **2005**, *307*, 569−573. (b) Lin, H.; Wagner, E. V.; Freemann, B. D.; Toy, L. G.; Gupta, R. P. *Science* **2006**, *311*, 639−642.

(5) (a) Huang, Y.; Dass, R. I.; Xing, Z.; Goodenough, J. B. *Science* **2006**, *312*, 254−257. (b) Berger, D. J. *Science* **1999**, *286*, 49.

(6) Volkl, J. In *Hydrogen in Metals I*; Alefeld, G., Volkl, J., Eds.; Springer-Verlag: Berlin, 1978; p 1.

(7) Yamauchi, M.; Kitagawa, H. *Synth. Met.* **2005**, *153*, 353−356.

(8) (a) Isobe, Y.; Yamauchi, M.; Ikeda, R.; Kitagawa, H. *Synth. Met.* **2003**, *135*, 757−758. (b) Ishimoto, T.; Tachikawa, M.; Yamauchi, M.; Kitagawa, H.; Tokiwa, H.; Nagashima, U. *Chem. Phys. Lett.* **2003**, *372*, 503−507. (c) Ishimoto, T.; Tachikawa, M.; Yamauchi, M.; Kitagawa, H.; Tokiwa, H;, Nagashima, U. J. *Phys. Soc. Jpn* **2004**, *73*, 1775−1780.

(9) (a) Yamamoto, Y.; Miumra, T.; Suzuki, M.; Nakamura, N.; Miyagawa, H.; Nakamura, T.; Teranishi, T.; Hori, H. *Phys. Rev. Lett.* **2004**, *93*, 116801. (b) Taniyama, T.; Ohta, E.; Sato, T. *Europhys. Lett.* **1997**, *38*, 195−200. (c) Shinohara, T.; Sato, T.; Taniyama, T. *Phys. Rev. Lett.* **2003**, *91*, 197201.

(10) (a) Haruta, M.; Kobayashi, T.; Sano, H.; Yamada, N. *Chem. Lett.* **1987**, *16*, 405−408. (b) Cambell, C. T. *Science* **2004**, *306*, 234−235.

(11) (a) Mutschele, T.; Kirchheim, R. *Scr. Metall.* **1987**, *21*, 1101. (b) Hanneken, J. W.; Suleiman, M.; Jisawai, N. M.; Dankert, O.; Reetz, M. T.; Bahts, C.; Kirchheim, R.; Pundt, A. J. *Alloys Compd.* **2003**, *356−357*, 644−648.

(12) Eastman, J. A.; Thompson, L. J.; Kestel, B. J. *Phys. Rev. B* **1993**, *48*, 84−92.

(13) (a) Natter, H.; Wettmann, B.; Heisel, H.; Hempelmann, R. J. *Alloys Compd.* **1997**, *253−254*, 84−86. (b) Rather, S.; Zacharia, R.; Hwang, S. W.; Niak, M.; Nahm, K. S. *Chem. Phys. Lett.* **2007**, *438*, 78−84. (c) Kuji, T.; Uchida, H.; Sato, M.; Cui, W. *J. Alloys Compd.* **1999**, *293−295*, 19−22. (d) Kuji, T.; Matsubara, Y.; Uchida, H.; Aizawa, T. *J. Alloys Compd.* **2002**, *330−332*, 718−722. (e) Kishore, S.; Nelson, J. A.; Adair, J. H.; Eklund, P. C. *J. Alloys Compd.* **2005**, *389*, 234−242.

(14) Wolf, R. J.; Lee, M. W.; Ray, J. R. *Phys. Rev. Lett.* **1994**, *73*, 557−560; Wolf, R. J.; Lee, M. W.; Davis, R. C. *Phys. Rev. B* **1993**, *48*, 12415−12418.

(15) Sachs, C.; Pundt, A.; Kirchheim, R.; Winter, M.; Reetz, M. T.; Fritsh, D.; *Phys. Rev. B* **2001**, *64*, 075408.

(16) Switendick, A. C. In *Hydrogen in Metals I, Basic Properties*; Alefeld, G., Volkl, J., Eds.; Springer-Verlag: Berin, 1978; p 101.

(17) Kubo, R. J. *Phys. Soc. Jpn.* **1962**, *17*, 975−986.

(18) (a) Teranishi, T.; Miyake, M. *Chem. Mater.* **1998**, *10*, 594−600. (b) Teranishi, T.; Miyake, M. *Hyomen* **1997**, *35*, 439.

(19) Wicke, E.; Brodowsky, H.; Züchner, S. *Hydrogen in Metals II, Application-Oriented Properties, Topics in Applied Physics*; Alefeld, G., Volkel, J., Eds.; Springer-Verlag: Berlin, 1978; Vol 29, p 73.

(20) Fukai, Y. *The Metal-Hydrogen System, Basic Bulk Properties*, 2nd ed.; Springer-Verlag: Berlin, 2005; pp 9−53.

(21) Le Bail, A.; Duroy, H.; Fourquet, J. L. *Mater. Res. Bull.* **1988**, *23*, 447−452.

(22) (a) Zanchet, D.; Telentino, H.; Martins, M. C.; Alves, O. L.; Ugarte, D. *Chem. Phys. Lett.* **2000**, *323*, 167−172. (b) Zang, P.; Sham, T. K. *Phys. Rev. Lett.* **2003**, *90*, 245502. (c) Page, K.; Proffen, T.; Terrones, H.; Terrones, M.; Lee, L.; Yang, Y.; Stemmer, S.; Seshadri, R.; Cheetham, A. K. *Chem. Phys. Lett.* **2004**, *393*, 385−388.

(23) (a) Eastman, D. E.; Cashion, J. K.; Switendick, A. C. *Phys. Rev. Lett.* **1971**, *27*, 35−38. (b) Papaconstantopoulos, D. A.; Klein, B. M.; Economou, E. N.; Boyer, L. L. *Phys. Rev. B* **1978**, *17*, 141−150. (c) Bakker, H. L. M.; Feenstra, R.; Griessen, R.; Huisman, L. M.; Venema, W. J. *Phys. Rev. B* **1982**, *26*, 5321−5332.

(24) Gelatt, C. D., Jr.; Ehrenreich, H.; Weiss, J. A. *Phys. Rev. B* **1978**, *17*, 1940−1957.

(25) Vuilemin, J. J.; Priestley, M. G. *Phys. Rev. Lett.* **1965**, *14*, 307. (b) Muller, F. M.; Freeman, A. J.; Dimmock, J. O.; Furdyna, A. M. *Phys. Rev. B* **1970**, *1*, 4617−4635.

(26) Schwarz, R. B.; Khachaturyan, A. G. *Phys. Rev. Lett.* **1995**, *74*, 2523−2526.

(27) (a) Gillespie, L. J.; Galstaun, L. S. *J. Am. Chem. Soc.* **1936**, *58*, 2565−2573. (b) Lee, T. D.; Yang, C. N. *Phys. Rev.* **1952**, *87*, 410−417. (c) Maeland, A. L.; Gobb, R. P., Jr. *J. Phys. Chem.* **1961**, *65*, 1270−1272. (d) Alefeld, G. *Phys. Status Solidi* **1969**, *32*, 67−80. (e) Alefeld, G.; Schaumann, G.; Tretkowski, J.; Völkl, J. *Phys. Rev. Lett.* **1969**, *22*, 697−700. (f) Buck, H.; Alefeld, G. 1972, *Phys. Status Solidi B* **1972**, *49*, 317−327.